4th International Conference on Molten Slags and Fluxes, 1992, Sendai, ISIJ

EFFECT OF SLAG FOAMING ON THE REDUCTION OF IRON OXIDE IN MOLTEN SLAG BY GRAPHITE

M. SHEIKHSHAB BAFGHI[1], Hirohide KURIMOTO[2] and Masamichi SANO[3]

1) Graduate School, Faculty of Engineering, Nagoya University, Furo-cho, Chikusa-ku, Nagoya, Aichi-ken, 464-01 Japan.
2) Formerly; Graduate School, Nagoya University, Now at Toho-Gas Co. Ltd., 19-18 Sakurada-cho, Atsuta-ku, Nagoya, 456, Japan.
3) Department of Materials Processing Engineering, Faculty of Engineering, Nagoya University. Japan

Synopsis

A kinetic study has been made on the reduction of iron oxide in molten slag with graphite, at 1300 ℃. The composition of the primary slag was 20.5%Li_2O-38.4%CaO-41.1%SiO_2. The initial FeO concentration varied between 3% and 12.5%. The rotation speed was changed from zero to 1900 rpm. The reaction rate was largely affected by slag foaming. At higher FeO concentrations, the apparent rate constant was almost independent of the mechanical stirring. At lower concentrations, the effect of the rotation on the apparent rate constant was small at lower speeds but became larger at higher speeds. This indicates that the melt was strongly agitated by bubble evolution. The effect of foaming is taken into account by introducing gas holdup factor into ordinary (foam-free) kinetic equations. Values of the mass transfer coefficient of oxygen in the molten slag, calculated by applying the penetration theory, are close to those of the apparent rate constant. This implies that the rate of the reduction is controlled predominantly by the mass transfer in the slag phase.

Key words: smelting reduction; FeO reduction; molten slag; solid graphite; slag foaming; kinetics; reaction mechanism; reduction rate.

1. Introduction

One of the very important features of smelting reduction is the slag foaming phenomenon. Although the phenomenon has been receiving due attention in recent years[1-5], however, the effect of slag foaming on the apparent rate constant has remained a matter of further study. In the present paper, results of kinetic experiments on the reduction of iron oxide in molten slag with graphite are discussed. Special attention is paid to the effect of slag foaming on the kinetics of the reaction. Efforts are made to find an appropriate way for considering the effect of slag foaming in kinetic analysis of the system.

2. Experimental

The apparatus is shown schematically in Fig. 1. A 5.5 kW SiC resistance furnace was used to melt the slag. Experiments were carried out by using an alumina crucible (O.D. 48 mm, I.D. 40 mm).

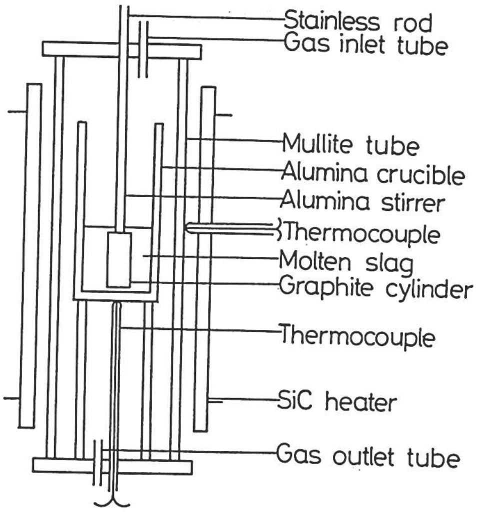

Fig. 1. Experimental apparatus.

Graphite was used in the form of cylinder, 1 cm in diameter and 4 cm in length.

The composition of the primary slag, before adding FeO, was $20.5\%Li_2O$-$38.4\%CaO$-$41.1\%SiO_2$ (molar ratio= 1:1:1).

Synthetic Fe_tO, hereinafter referred to as iron oxide or simply FeO, was prepared by melting a mixture of reagent Fe_2O_3 and electrolytic iron powders in an iron crucible under the argon gas atmosphere.

The weight of the primary slag used for each experiment was 75 g. All the experiments were carried out at 1300 ℃, under argon gas atmosphere (flow rate ~ 1000 cm^3/min). When the primary slag was melted and temperature reached to the desired level, iron oxide was added to the melt. The initial FeO concentration varied from 3% to 12.5%. After the iron oxide was melted and the composition was homogenized, graphite cylinder was immersed into the melt and rotation was started. The rotating speed varied from zero to 1900 rpm.

Sampling was done by means of long nickel rods dipped into the melt at appropriate time intervals. The height of slag phase was obtained by measuring the height of sample attached to the nickel rod.

3. Results

During the period of the first 1 min, the slag phase swelled very rapidly. This indicates that the kinetics of the reaction during this period differs from that in the foamed slag. Therefore, the starting point for the kinetic analysis was set at 1 min after immersing the graphite cylinder into the molten slag. FeO concentration pertaining to this point was shown as $(\%FeO)_i$ and is referred to as initial concentration, hereinafter.

Typical FeO concentration-time curves for various initial FeO concentrations are shown in Fig.2. This figure shows that the rate of reduction ($-d(\%FeO)/dt$) is dependent on the initial FeO concentration. From the figure it is also seen that for the initial FeO concentrations above 4%, the rate of reduction decreases as the initial FeO concentration increases. This behavior is assumed to be due to the slag foaming.

Figure 3 shows the variation of slag height with time. The height of slag phase increases as initial FeO concentration increases. The average height of slag phase from 1 to 6 min increases with increasing initial iron oxide concentration, as shown in Figure 4. When the FeO initial concentration is below 3%, the slag remains almost free of foam.

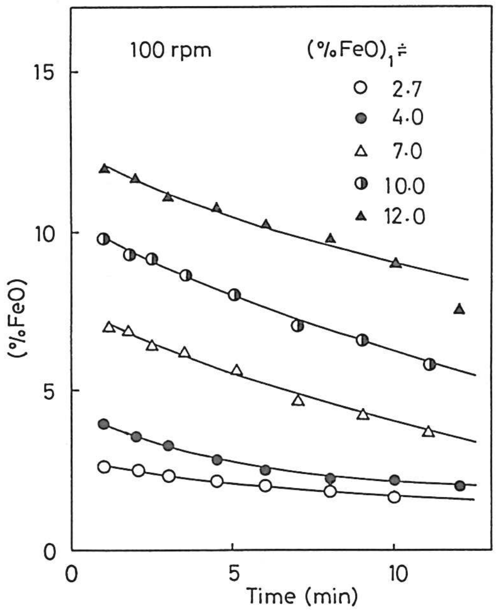

Fig. 2. FeO concentration in slag vs. time.

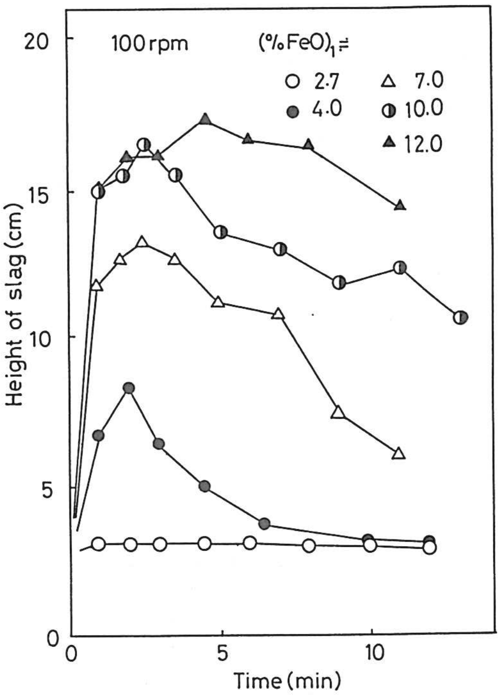

Fig. 3. Height of slag vs. time.

4. Kinetic equation

Plots of ln(%FeO) against time for various initial FeO concentrations showed that the apparent order of the reaction, with respect to the iron oxide concentration could be taken as unity. Hence, assuming FeO concentration at the interface is zero, kinetic equation will be

$$-\mathrm{d}\ln(\%\mathrm{FeO})/\mathrm{d}t=kA/V_S \qquad (1)$$

where k, A and V_S, respectively, are the apparent rate constant, interfacial area and volume of the slag.

If the effect of slag foaming is neglected (case A), then,

$$V_S=V_D \qquad (2)$$

$$V_D=W_S/\rho_s \qquad (3)$$

where, V_D, W_S and ρ_s, respectively, are the volume of dense (foam-free) slag and weight and density of the slag.

Hence, in case of foam-free assumption, the kinetic equation will be

$$-\mathrm{d}\ln(\%\mathrm{FeO})/\mathrm{d}t=k_AA/V_D \qquad (4)$$

where, k_A is the apparent rate constant for the foam-free kinetic treatment.

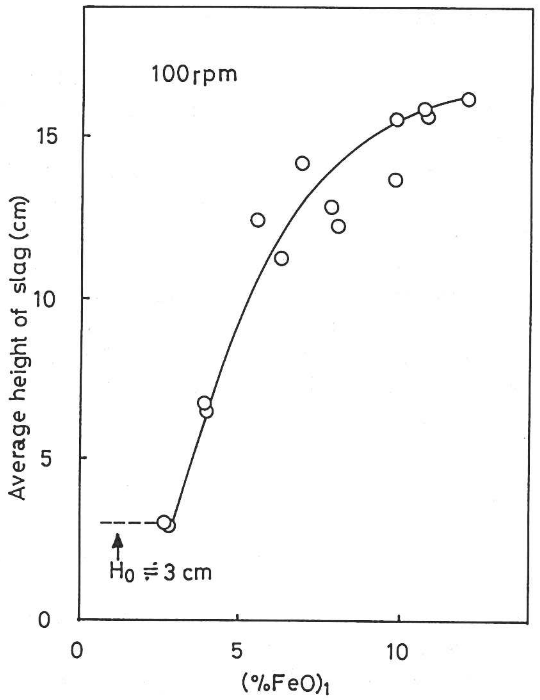

Fig. 4. Relation between the average height of slag and (%FeO)$_1$.

But, if the effect of foaming is considered (case B), the volume of the slag will be

$$V_S=A_Dh_{av} \qquad (5)$$

where, A_D and h_{av} are the cross sectional area of crucible and average height of slag, respectively.

Combining Eqs. (1) and (5), Eq. (6) is obtained as the kinetic equation for case B.

$$-\mathrm{d}\ln(\%\mathrm{FeO})/\mathrm{d}t=k_BA/A_Dh_{av} \qquad (6)$$

where, k_B is the apparent rate constant for the real foamed system.

Relation between the apparent rate constants of the two cases is given by Eq. (7).

$$k_B=k_A/(1-\varepsilon) \qquad (7)$$

where, gas holdup factor, ε, is the ratio of the volume of gas contained in slag ($V_g=V_s-V_D$) to the total volume of foamed slag (V_s),

$$\varepsilon=V_g/V_S=1-V_D/V_S. \qquad (8)$$

Combining Eqs. (3), (5) and (8), one obtains

$$\varepsilon=1-W_S/(\rho_sA_Dh_{av}). \qquad (9)$$

5. Discussion

5.1. Effect of foaming phenomenon

Figure 5 shows the relation between the apparent rate constant and the initial concentration of iron oxide. Here, Eq. (1) was applied to obtain the apparent rate constant. From Fig. 5, it is clear that the apparent rate constant decreases when the initial iron oxide concentration exceeds about 6%. This apparently strange behavior is supposed to be due to the foaming phenomenon. Considering the effect of foaming, the apparent rate constant is calculated by applying Eq. (6). Figure 6 shows the relation between the apparent rate constant, k_B, and initial FeO concentration. No strange behavior is observed in this figure. This indicates that in kinetic analysis of the foaming systems, due corrections must be made by introducing gas holdup factor into the ordinary (foam-free) kinetic equations. Figure 6 shows that when the initial concentration of iron oxide increases from 2.5% up to 5.5%, the apparent rate constant increases. Above 5.5% it remains almost constant. These phenomena are presumed to be due to the convective agitation by CO gas evolution and/or to the compulsory neglect of the gas holdup in the vicinity of the graphite cylinder at initial FeO concentrations below 3%. This will be discussed later.

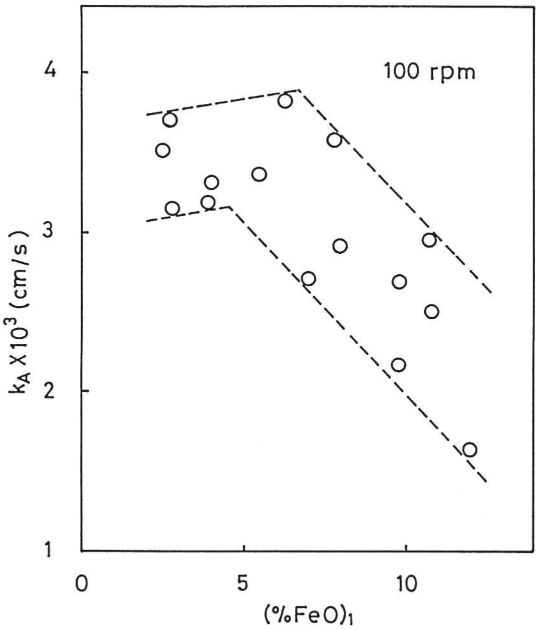

Fig. 5. Apparent rate constant as a function of $(\%FeO)_i$ (case A).

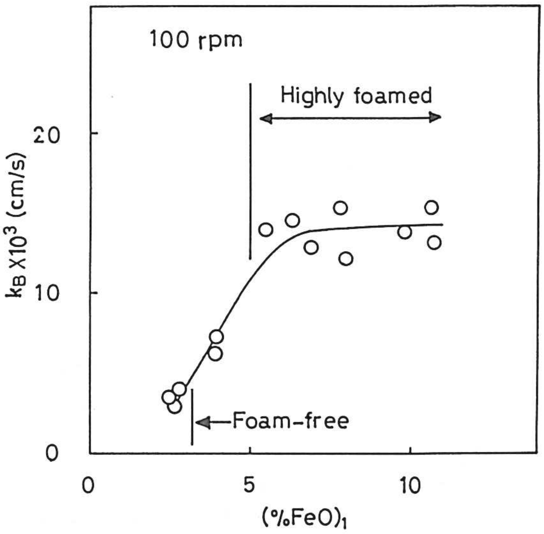

Fig. 6. Apparent rate constant as a function of $(\%FeO)_i$ (case B).

5.2. Reaction mechanism

Since the apparent order of the reaction is unity, it is reasonable to start the kinetic analysis with a mass transfer-control assumption.

If mass transfer in the slag phase controls the rate of the reduction, an increase in the apparent rate constant would be expected when the melt is agitated. In this case, the effect of agitation becomes higher as FeO concentration decreases. In Fig. 7 the apparent rate constant is plotted against the rotation speed of the graphite cylinder. As seen in this figure, dependency of the apparent rate constant on the rotation speed of the graphite cylinder is tangible only at lower concentrations. This figure also shows that the dependency of the apparent rate constant on the rotation is small at lower speeds but tends to become larger at higher speeds.From this fact it can be concluded that convective agitation, caused by evolution

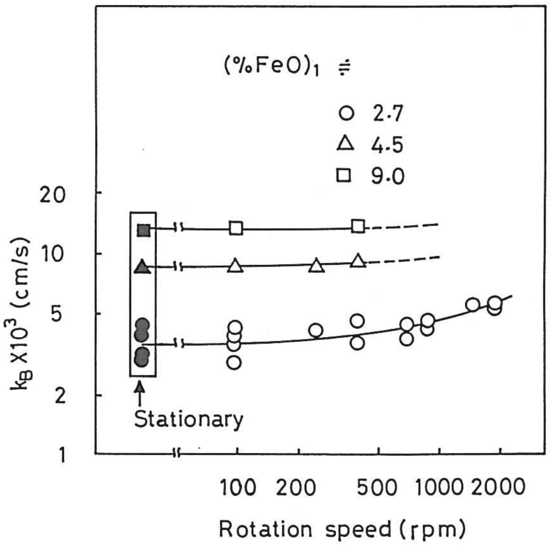

Fig. 7. Relation between the apparent rate constant (k_B) and rotation speed.

of the CO gas bubbles, is so strong that the effect of mechanical stirring is not perceptible, especially at higher FeO concentrations and at lower rotation speeds.

In a system agitated by bubble evolution at the interface, convective mass transfer coefficient, k_m, can be calculated by using Eq. (10), which is a result of the well-known surface penetration theory.

$$k_m=2(D/\pi t_c)^{1/2} \qquad (10)$$

where, D and t_c are diffusivity and time of the surface renewal, respectively.

Here, t_c is assumed to be equal to the time of bubble formation at the interface. By calculating the rate of CO gas generation, which is identical to the rate of FeO reduction, t_c could be calculated. Doing so, and assuming $d(\%FeO)/dt \fallingdotseq \Delta(\%FeO)/\Delta t$ for the first stage of the reaction up to 6 min, then under the conditions of the present study

$$k_m \fallingdotseq 6.61[(W_s/d_c^3)(-\Delta\%FeO/\Delta t)D]^{1/2} \qquad (11)$$

where, d_c is the critical diameter of the bubble.

Since the diffusivity of iron ion is much larger than that of oxygen ion[6], therefore, if mass transfer has any control over the rate of reaction, that is in fact transfer of oxygen ions which controls the rate. Johnston et al.[7] have argued that the effect of thermodynamic gradient on the diffusion coefficient is small and hence, self-diffusivity data may be used in mass transfer calculations without introducing significant error. So, one can assume that

$$D_O \fallingdotseq D^*_O \qquad (12)$$

where, D_O and D^*_O are the chemical- and self-diffusivities of oxygen, respectively.

The self-diffusivity can be approximated by applying Stokes-Einstein equation,

$$D^*_i=kT/6\pi r_i \eta \qquad (13)$$

where, k, T, r_i and η, respectively are the Boltzmann constant, temperature in K, atomic radius of the diffusing constituent and viscosity of the medium.

Slag viscosity has been calculated by applying Bottinga and Weill's model[9],

$$\ln\eta=\Sigma N_i \eta_i \qquad (14)$$

where, N_i is the mole fraction of the component i and η_i is an empirical constant associated with this component.

Comparison between the experimental values of the viscosity of SiO_2-Li_2O slags[9] and those calculated from Eq. (14) showed a good agreement and proved that this model can reliably be applied to calculate the slag viscosity.

Koros and King[10] have measured the diffusivity of oxygen in a liquid silicate (40%SiO_2-40%CaO-20%Al_2O_3). Comparison between the diffusivities calculated in the present work to those obtained by Koros and King showed a very good agreement. This confirms the reliability of the calculated diffusivities.

Equation (11) shows that bubble diameter has a large effect on the calculated mass transfer coefficient and, hence, it should be carefully estimated. From the direct observations of the bubble size during the course of reduction and also by referring to the X-Ray photographs, bubble diameter was estimated to be about 5 mm.

The apparent rate constant (k_B) and the calculated mass transfer coefficient (k_m) for various iron oxide concentrations are shown in Table 1. As seen in the table, for FeO concentrations higher than 3%, values of the apparent rate constant are closed to those of the mass transfer coefficient. This reveals that the rate of reduction is controlled by the mass transfer in the slag phase. When initial iron oxide concentration is below 3%, the mass transfer coefficient is larger than the apparent rate constant. As mentioned earlier, for FeO concentrations lower than 3%, the slag bulk remains dense. Nevertheless, evolution of the CO gas is clearly evident during the course of the reaction. Therefore, the slag in the vicinity of the graphite cylinder is no longer dense. In this case it is impossible to estimate the gas holdup factor from the height of slag attached to the sampling rod and hence, the apparent rate constant must be calculated with the assumption of a foam-free boundary layer. This means that the effect of the gas holdup in the vicinity of the interface is reflected on the apparent rate constant. With iron oxide concentrations above 4%, the slag is supposed to be fully foamed and gas holdup near the interface is almost the same as in the slag bulk. Therefore, gas hold up factor can be evaluated from the height of the foamed slag, for correcting the apparent rate constant.

In calculating k_B from Eq. (6), contribution of the indirect reduction by CO gas was neglected. If this is taken into account, somewhat lower values are obtained for k_B. Also, in deriving Eq. (11) for the calculation of the mass transfer coefficient, the frequency of the surface renewal was assumed to be equal to the bubble formation frequency. This, implicitly, means that each individual bubble affects the whole slag around the contact area. Because of this, mass transfer coefficients might have been overestimated. Nevertheless, the apparent rate constant, k_B, remains higher than the calculated mass transfer coefficient, which means the reaction rate is under the control of the mass transfer in the slag phase.

Table 1: Kinetic characteristics with various FeO concentrations.

$(\%FeO)_1$	ε	$k_B \times 10^3$ (cm/s)	$k_m \times 10^3$ (cm/s)
12.0	0.82	8.86	10.00
10.7	0.81	15.29	12.49
9.8	0.81	13.90	12.54
9.8	0.78	9.82	11.12
8.0	0.76	12.10	12.47
7.8	0.77	15.28	12.41
6.9	0.79	12.74	11.11
6.3	0.74	14.58	12.00
5.5	0.76	13.96	10.47
4.0	0.54	7.28	9.75
2.8	~ 0	4.00	7.59
2.7	~ 0	2.87	6.07
2.5	~ 0	3.50	6.03

7. Conclusions

1) In kinetic analysis of the reduction of iron oxide in molten slag by solid carbon, due consideration must be given to the effect of foaming.

2) In kinetic analysis of foaming systems, effect of foaming can be taken into account by introducing gas holdup factor into the ordinary (foam-free) kinetic equations.

3) Values of the mass transfer coefficient, calculated by applying penetration theory, are close to the values of the apparent rate constant measured experimentally. This implies that the rate of reduction is controlled by the mass transfer in the slag phase.

References:

1) K.Ito and J.R.Fruehan: Metall. Trans. B, 20B(1989), 509.
2) K.Ito and J.R.Fruehan: Metall. Trans. B, 20B(1989), 515.
3) R.Jiang and R.J.Fruehan: Metall. Trans. B, 22B(1991), 481.
4) Y.Ogawa, H.Katayama, H.Hirata, N.Tokumitsu and M.Yamauchi: Trans. Iron steel Inst. Jpn., 32(1992), 87.
5) S.Hara and K.Ogino: Trans. Iron steel Inst. Jpn., 32(1992), 81.
6) D.P.Agarwal and D.R.Gaskell: Metall. Trans. B, 6B(1975), 263.
7) R.F.Johnston, R.A.Stark and J.Taylor: Ironmaking Steelmaking, 1(1974), 220.
8) Y.Bottinga and D.F.Weill: Am. J. Sci., 272(1972), 438.
9) J.O'M.Bockris, J.D.Mackenzie and J.A.Kitchener: Trans. Faraday Soci., 151(1955), 1734.
10) P.J.Koros and T.B.King: Trans. Metall. Soc. AIME, 224(1962), 299.